Utilizing Numerical Simulations to Analyze the Efficiency of a Porous Reactor

Wilson Ribeiro do Prado Júnior
Department of Basic Science and Environmental
Engineering School at Lorena, University of São Paulo
Lorena, São Paulo, Brasil
wrpjunior@usp.br

Jairo Aparecido Martins
Research & Development
DESCH North America
Cambridge, Ontario, Canada
Jairo.martins@desch.com

Estaner Claro Romão
Department of Basic Science and Environmental
Engineering School at Lorena, University of São Paulo
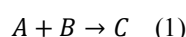Lorena, São Paulo, Brasil
estaner23@usp.br

Abstract-This paper presents a series of numerical simulations of a porous reactor, where a generic reaction between reagents is carried out, generating a product. All numerical simulations were performed by using the software COMSOL Multiphysics, which made use of the Navier-Stokes and Brinkman equations. These equations were utilized to govern the fluid flow in the numerical simulation. Throughout the simulations, several initial parameters were altered to evaluate their impact on the reactor efficiency based on the concentration of component C. Furthermore, other parameters such as the distribution of speed and geometry in the equipment were taken into consideration, and an optimal configuration for the case is demonstrated.

Keywords-numerical simulation; porous reactor; Navier-Stokes equations; brinkman equations

I. INTRODUCTION

This works aims to study the effects of some process parameters in a reactor of porous media, to provide industrial improvements, and to maximize the obtained product for the same reactor or similar equipment. Although the type of reactor studied in this work has several applications for expelling gas into the atmosphere, it is treated in a generic manner in order to reach a conclusion and extend it to any similar reactor. As an example, this type of reactor has several applications in industries, including internal combustion engines [1-3] where the post-treatment of exhausted gases can be numerically simulated [4-7]. In this paper, a generic case is assumed with a simple chemical equation to analyze this type of reactor, and the way its properties influence its performance, when the species A and B react to form the species C:

$$A + B \rightarrow C \quad (1)$$

Since this reaction only occurs in a porous catalyst and the intention is to treat generic cases, the initial porosity is assumed as 0.3 and fixed with a low permeability established as 10^{-9}, comparable with the permeability of brick or leather, which are in the range of 10^{-9} to 10^{-10}. This paper uses a modeled reactor with porous media as provided by COMSOL^{TM}, with the adaptation shown in Figure 1.
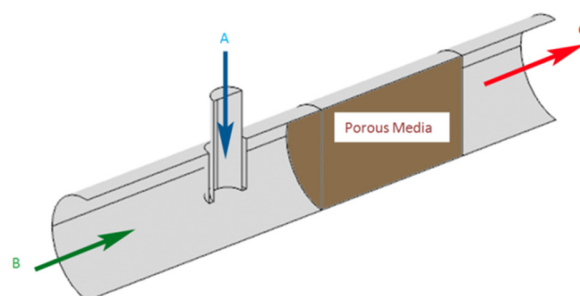

Fig. 1.   Model of the reactor of porous media showing the inlet and outlet.

This paper's main idea is to numerically simulate the process of heterogeneous catalyzing between two species of reagents. It happens when the species A is injected into a reactor through a perpendicular tube while the species B gets into the tube by the tube's main entrance (Figure 1). Both are partially mixed into the reactor before they pass through the porous media, where a reaction occurs and the third species C is obtained. This reaction happens with the transport of ideally inert gas in the reaction. So, it is expected with the simulations and improvements implemented to decrease the concentration of the species B being expelled out of the equipment. As described previously, this type of reactor can be utilized in combustion engines to reduce gas emissions to the atmosphere. Further, several equations that govern the phenomenon are presented, also the main parameters utilized (chemical reaction, system geometry, mesh, etc.), and lastly, the obtained output is

shown. In addition, this work shows the way the sequence of analysis of the parameters is involved in the problem and the consequent optimization can bring benefits to the process and the economy by reducing operating costs.

II.   FLOW IN POROUS MEDIA

A. Transport of Diluted Species

A diluted species has a very small concentration when compared with a solvent fluid. Consequently, mixture properties such as density and dynamical viscosity may be considered equal to the solvent's. The equation of mass conservation used to calculate the transport of diluted species by diffusion and convection is given by [9]:

$$\frac{\partial C_i}{\partial t} + \nabla \cdot J_i + u \cdot \nabla C_i = R_i \quad (2)$$

where C_i is the species concentration (mol/m³), R_i is the reaction rate of species i (mol/(m³·s)), u is the fluid median velocity (m/s) and J_i is the diffusive flow vector (mol/(m²·s)).

B. Brinkman's Equations

Brinkman's equations are an extension of Darcy's equation that describes the movement of a slow flow in porous media. It describes the dissipation of kinetic energy by the viscous shearing from Navier-Stokes equations, which describes the fast-flow movements throughout free channels. So, these equations calculate the fast movements of fluids in porous media with kinetic potential by velocity, pressure, and gravity into the flow. The flow in porous media is governed by the equation of continuity and momentum, converging to Brinkman's equation [9]:

$$\frac{\partial}{\partial t}(\varepsilon_p \rho) + \nabla \cdot (\rho u) = Q_m \quad (3)$$

$$\frac{\rho}{\varepsilon_p}\left(\frac{\partial u}{\partial t} + (u \cdot \nabla)\frac{u}{\varepsilon_p}\right) = -\nabla p + \nabla \cdot \left[\frac{1}{\varepsilon_p}\left\{\mu \nabla u + (\nabla u)^T - \frac{2}{3}\mu(\nabla \cdot u)I\right\}\right] - \left(\kappa^{-1}\mu + \frac{Q_m}{\varepsilon_p^2}\right)u + F \quad (4)$$

where μ is the dynamic viscosity of the fluid (kg/(m·s)), u is the velocity vector, ρ is the density of the fluid (kg/m³), p is the pressure (Pa), ε_p is the porosity, κ is the permeability of the porous medium (m²), and Q_m is a mass source or sink (kg/(m³·s)).

III.   MODELING THE PHENOMENA

The model for the phenomena of transport to diluted species utilized here is composed of the Navier-Stokes and Brinkman equations (as mentioned above). Here, an isothermal situation is adopted and the used gas transported is Nitrogen. In terms of geometry, it complies with Figure 2, where: $H = 0.01$, $R = 0.01$, $H_p = 0.003$, $Ra = 0.0004$, $Ha = 0.002$, $Rai = 0.0002$, $D = 0.005$, $d = 0.003$ (all in meters), that will be used in Case 1. In terms of mesh building, the physical type of the element was considered, therefore, the "normal" mesh type was used, which has 166,645 domain elements, 16,556 boundary elements, and 758 edge elements. It is important to highlight that this work does not aim at a particular reaction, but rather a generic case is demonstrated. Although in this simulation the kinetics of the reaction is governed by a generic equation, it is important to

understand that a specific and real case requires a particular kinetics analysis. The expression that follows is the one utilized in this paper for the generic analysis:

$$R_C = A_f \cdot e^{\left(-\frac{E}{Rg \cdot T_{iso}}\right)} \cdot C_A \cdot C_B \quad (5)$$

where R_C is the formation rate of species C (mol/(m³·s)), A_f is the frequency factor (m³/(s·mol)), E is the activation energy (J/mol), Rg is the universal constant of gases (J/(mol·K)), T_{iso} is the isothermal temperature of reaction (K), C_A and C_B are the concentrations (mol/(m³·s)).
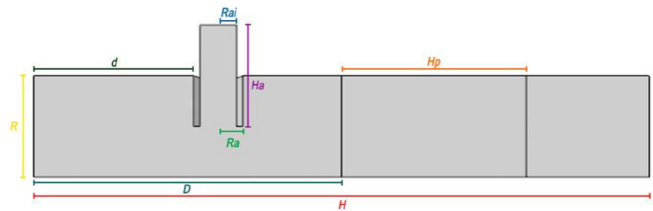

Fig. 2.   Geometric parameters of the reactor.

IV.   RESULTS AND DISCUSSION

Even though the presented simulations came from innumerable combinations of the concentrations as inlets for each species, the velocity of each species, the adopted isothermal conditions, and the area of the region where the mixture occurs (Hp), only the main results are presented in the paper.

A. Case 1

For this case, the following parameters are considered: $\varepsilon = 0.3$, $\kappa = 10^{-9}$ m², $v_A = 0.025$ m/s (velocity of input A), $v_{B_2} = 0.025$ (velocity of input B), $Df_a = Df_b = Df_c = 10^{-6}$ m²/s (diffusion coefficient of the species), $C_A = 7$ mol/m³ (initial concentration of species A) and $C_B = 1$ mol/m³ (initial concentration of species B). The concentration of species B (Figure 3) is homogeneously distributed in the reactor, except in the entrance duct of species A, where the concentration is zero. We notice that in the upper part of the reactor inside and just after the porous media where the concentration of B drops approximately to 0.7 mol/m³. Albeit this happens due to the system reaction, the lower part of the reactor remains practically the same as the initial concentration.
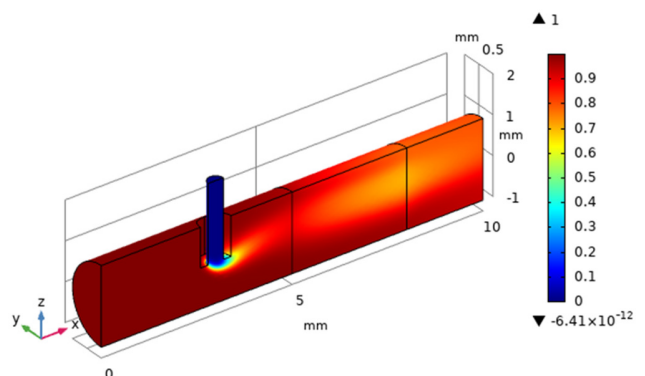

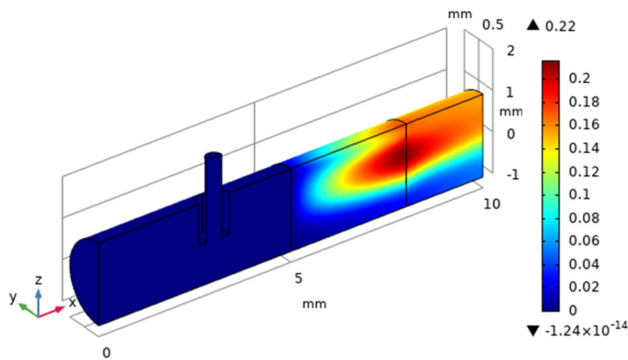Fig. 3.   Case 1: Distribution of the concentration of species B (mol/m³).

Fig. 4.   Case 1: Distribution of the concentration of species C (mol/m³).

The way the reaction happens is shown in Figure 4. In the upper part of the reactor, almost there isn't any formation of species C in the lower region. This matches with the result presented in Figure 2, where species B has its concentration reduced in the upper region of the reactor. Note that, soon after the porous media, species C starts to become homogeneous in the solution. By the dimension of the high of the duct (Figure 5), it is possible to observe with more precision the concentration of the species B in the outlet of the reactor, which is between 0.78 mol/m³ and 0.94 mol/m³. Taking into consideration that the main objective of the process is to have the reduced concentration of the species B expelled from the reactor, it is not so efficient, since the substance entered the reactor where the initial concentration was 1 mol/m³ and had a maximum reduction of 20%.
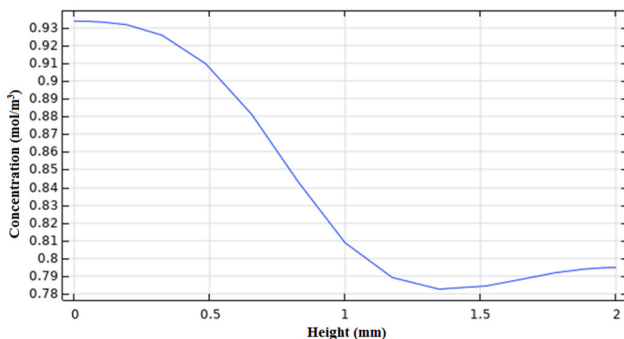

Fig. 5.   Case 1: Concentration of species B in the reactor outlet.

B. *Case 2*

Compared with Case 1, a change in velocity of v_A = 0.075 m/s is adopted. The increase of the entrance velocity of species A in the reactor resulted in the consumption of species B being much more pronounced than verified in Figure 6. Nevertheless, since the duct entrance radius was kept the same, it resulted in a raise of the velocity and consequently a proportional increase of the flow of species A, which means that 3 times more reagent A would be required to produce a change in concentration. This condition is not satisfactory since it would end up elevating the cost of the process.
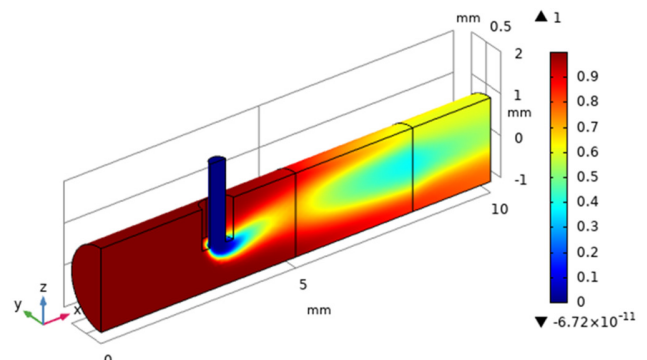

Fig. 6.   Case 2: Distribution of the concentration of species B (mol/m³).

C. *Case 3*

Compared with Case 1, here the C_A is assumed to be 10 mol/m³. In this case, changing only the C_A, resulted in a highly reduced variation of the limits presented in Figures 5 and 7. This means that the superior limit of approximately 0.94 changed to 0.92 mol/m³, and the inferior limit from 0.78 to 0.74. Both generate a very small "gain" when compared with an increase in the concentration of the species A.
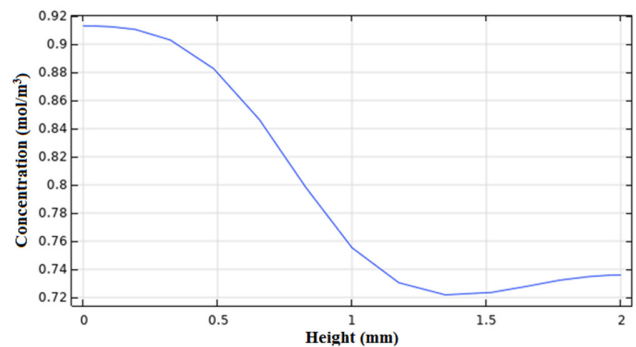

Fig. 7.   Caso 3: Concentration of species B in the reactor outlet.

D. *Case 4*

In this simulation a change of T_{iso} = 400 K is adopted.
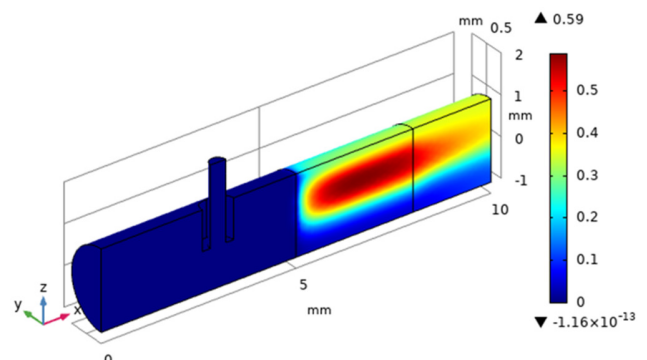

Fig. 8.   Case 4: Distribution of the concentration of species C (mol/m³).

An increase of the temperature (isothermal) in the system favors the reaction (Figure 8), raising substantially the

generation of a species C, which reaches close to triple its value at its maximum point, 0.59 mol/m^3 versus 0.22 mol/m^3 in the parameter of Case 1. However, high heating, with an increase of 100 ^{o}C might be costly and even making unfeasible to build a reactor due to the needed material thermal properties requirements.

E. Case 5

In this simulation a change of H_p = 4 mm is adopted. Likewise Case 3, this case (Figure 9) does not result in an expressive benefit in the decreasing of the species B in the reactor outlet, but still ends up with an increase of 33% in the size of the porous region.
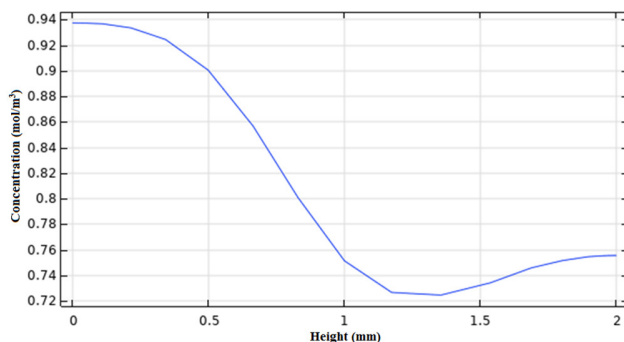

Fig. 9.　　Case 5: Concentration of species B in the reactor outlet.

F. Case 6

In this simulation, a change of d = 1 mm is adopted. An increase in the distance of entrance of species A (Figure 10) towards the porous media in the reactor almost does not bring change to the process, even though it helps in the homogenously of the solution, which can be seen by the concentration of the species C. The formation happens in a more distributed shape in the porous media.
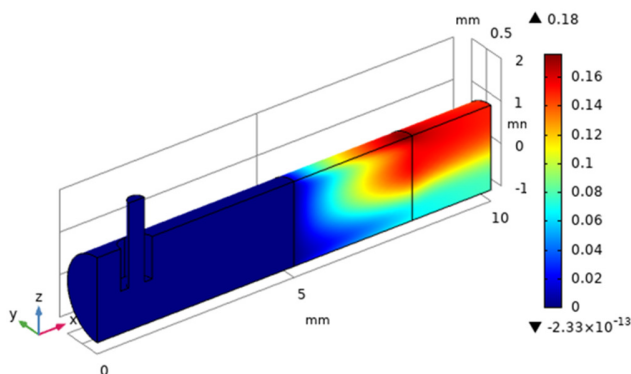

Fig. 10.　　Case 6: Distribution of the concentration of species C (mol/m^3).

G. Optimization

Although most of the considered changes brought positive advantages, those resulted in a cost increase on the project coming from more expensive materials needed to build the reactor. This happens because the reactor had to withstand either extreme conditions or a considerable jump in the energy

consumption or the reagents. A possible solution tested was to add these changes on a reduced scale, indeed, increasing the velocity of entrance of the species A by 0.05 m/s rather than tripling its value. Making use of the following parameters: v_A = 0.030 m/s, C_A = 8 mol/m³, Ra = 0.45 mm, Rai = 0.25 mm, T_{iso} = 350 K, Hp = 3.5 mm, d = 1 mm, the results are presented in Figure 11.
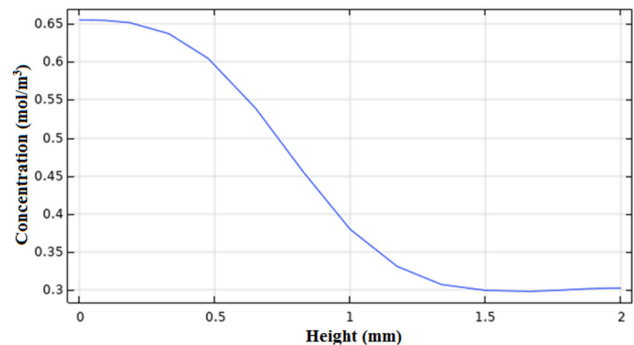

Fig. 11.　　Optimization: Concentration of species B in the reactor outlet.

The results are satisfactory since a reduction of the concentration of B of approximately 50% can be obtained when compared with the inlet concentration.

V.　CONCLUSIONS

This paper made use of many numerical simulations to analyze the way the geometrical and physical-chemical properties of a reactor of porous media could influence its efficiency, analyzing them separately or in a group. It was concluded that many of the changes suggested resulted in good results or at least some impact on the reactor operation manner. However, many of them bring problems with applications like a need for more specific and expensive materials to build the reactor, something that ends up as economically unfeasible. By applying minor changes in the parameters that could result in a decrease in the residual concentration of species B, the process was optimized rather than opting for a change in only one parameter.

REFERENCES

[1] M. Weclas, "Potential of Porous-Media Combustion Technology as Applied to Internal Combustion Engines," *Journal of Thermodynamics*, vol. 2010, Feb. 2011, Art. no. e789262, https://doi.org/10.1155/2010/789262.

[2] Z. G. Deng, R. Xiao, B. S. Jin, Q. L. Song, and H. Huang, "Multiphase CFD Modeling for a Chemical Looping Combustion Process (Fuel Reactor)," *Chemical Engineering & Technology*, vol. 31, no. 12, pp. 1754–1766, 2008, https://doi.org/10.1002/ceat.200800341.

[3] A. Abad, J. Adánez, L. F. de Diego, P. Gayán, F. García-Labiano, and A. Lyngfelt, "Fuel reactor model validation: Assessment of the key parameters affecting the chemical-looping combustion of coal," *International Journal of Greenhouse Gas Control*, vol. 19, pp. 541–551, Nov. 2013, https://doi.org/10.1016/j.ijggc.2013.10.020.

[4]   W. A. Cutler, "Overview of Ceramic Materials for Diesel Particulate Filter Applications," in *28th International Conference on Advanced Ceramics and Composites A: Ceramic Engineering and Science Proceedings*, 2004, pp. 421–430, https://doi.org/10.1002/97804702911 84.ch61.

[5]   J. P. Muhirwa, S. I. Mbalawata, and V. G. Masanja, "Markov Chain Monte Carlo Analysis of the Variable-Volume Exothermic Model for a Continuously Stirred Tank Reactor," *Engineering, Technology & Applied Science Research*, vol. 11, no. 2, pp. 6919–6929, Apr. 2021, https://doi.org/10.48084/etasr.3962.

[6]   H. A. Maddah, "Numerical Analysis for the Oxidation of Phenol with TiO2 in Wastewater Photocatalytic Reactors," *Engineering, Technology & Applied Science Research*, vol. 8, no. 5, pp. 3463–3469, Oct. 2018, https://doi.org/10.48084/etasr.2304.

[7]   S. Bekkouche and M. Kadja, "Numerical Analysis of Density-Driven Reactive Flows in Hele-Shaw Cell Geometry," *Engineering, Technology & Applied Science Research*, vol. 10, no. 2, pp. 5434–5440, Apr. 2020, https://doi.org/10.48084/etasr.3349.

[8]   D. A. Nield and A. Bejan, *Convection in Porous Media*. New York, NY, USA: Springer, 2013.

[9]   *Subsurface Flow Module User's Guide v. 5.5*. Stockholm, Sweden: COMSOL, 2020.